External charge state detection of a double-dot system

Islamshah Amlani,[a] Alexei O. Orlov, Gregory L. Snider, Craig S. Lent, and Gary H. Bernstein
Department of Electrical Engineering, University of Notre Dame, Notre Dame, Indiana 46556

(Received 30 May 1997; accepted for publication 25 July 1997)

We report direct measurements of the charging diagram of a nanoscale series double-dot system at low temperatures. Our device consists of two metal dots in series, with each dot capacitively coupled to another single dot serving as an electrometer. This configuration allows us to externally detect all possible charge transitions within a double-dot system. In particular, we show that transfer of an electron between two dots, representing a polarization switch of the double dot, can be most prominently detected by our differential sensing scheme. We also perform theoretical calculations of the device characteristics and find excellent agreement with experiment. We discuss possible applications as an output stage for quantum-dot cellular automata architecture. © *1997 American Institute of Physics.* [S0003-6951(97)00738-9]

Recently, there has been a growing interest in coupled mesoscopic structures utilizing the Coulomb blockade (CB) phenomenon for their possible applications as electronic devices.[1–6] Various investigators have pointed out that coupled dots in the CB regime can perform useful computing functions.[7–13] A revolutionary computational paradigm, known as quantum-dot cellular automata (QCA), depends on the ability to control and detect the position of single electrons in an array of coupled dots to perform digital computation.[8–11] The basic building block of QCA is a four dot cell shown in Fig. 1. A QCA cell can be constructed of two series-connected dots separated by tunneling barriers and capacitively coupled to a second, identical double dot. If the capacitances are sufficiently small, charge is quantized on the dots.[1]

If the cell is biased such that there are two excess electrons within the four dots (one excess electron per double dot), these electrons will be forced to opposite ''corners'' of the four-dot system by Coulomb repulsion. The two possible electron configurations, i.e., the polarization states of the system, represent logic ''0'' and ''1,'' as depicted in Fig. 1. Properly arranged, arrays of these basic cells can perform Boolean logic functions.

Critical to the implementation of QCA is a means of detecting the positions of individual electrons in the output cells. It has been shown[14,15] that a metal dot can be used to detect charge variation in another nearby dot. In previous double-dot experiments, the Coulomb interaction of electrons within two-dot systems is inferred exclusively from their charging diagrams.[4–6] A detection scheme that can probe the polarization state of the double dot externally, and with high sensitivity, has not heretofore been reported.

We present direct measurement of the internal charge state of a double-dot system. Specifically, we show that our charge detection technique is sensitive not only to the charge variation of individual dots but also to the more subtle exchange of one electron between the two dots. Our experimental results exhibit excellent agreement with theory. By showing that switching of an electron within a double dot can be externally detected, we demonstrate that our detection scheme is suitable for sensing the polarization state of a QCA cell.

Figure 2 shows a schematic diagram of our experiment. The device under study consists of four Al islands referred to as dots D_1, D_2, D_3, and D_4, respectively. Dots D_1 and D_2 are connected by a tunnel junction and are capacitively coupled to dots D_3 and D_4 which serve as electrometers. Dots D_1 and D_2 are also capacitively coupled to control gates A and B, respectively, to change the electron populations of their respective dots. In the experiment, we use control gates to shift an electron from D_1 to D_2 or vice versa, mimicking a QCA transition, and measure the conductances of D_3 and D_4 simultaneously as a function of bias on the control gates.

Fabrication of $Al/AlO_x/Al$ tunnel junctions is accomplished using standard electron beam lithography procedure and double angle shadow evaporation of Al.[16] The bottom electrode metal, 25 nm thick, is oxidized *in situ*, followed by 50 nm of Al to form the top electrode. The two islands, labeled D_1 and D_2 in Fig. 1, between the three ($60 \times 60\ nm^2$) tunnel junctions are 1.4 μm long, and the lengths of islands D_3 and D_4 are 1.1 μm each.

The sample is mounted on the cold finger of a dilution refrigerator with a base temperature of 25 mK. Conductances of the double dot and each electrometer are measured simultaneously using standard ac lock-in techniques with an excitation voltage of 4 μV at 16–40 Hz. A magnetic field of 1 T is applied to suppress the superconductivity of Al. The typical tunnel resistance of a junction, based on I–V measurements of the electrometers at 1 K, is approximately 200 kΩ. The total capacitance of the electrometer dots, C_Σ, extracted from the charging energy ($E_C \sim 80\ \mu eV$), is approximately 1 fF. Various lithographic and parasitic capacitances between different gates and islands are determined from the period of

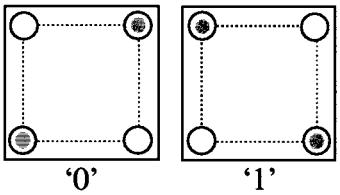

FIG. 1. QCA cell showing the two possible polarizations.

[a]Electronic mail: Islamshah.amlani.1@nd.edu

 0003-6951/97/71(12)/1730/3/$10.00

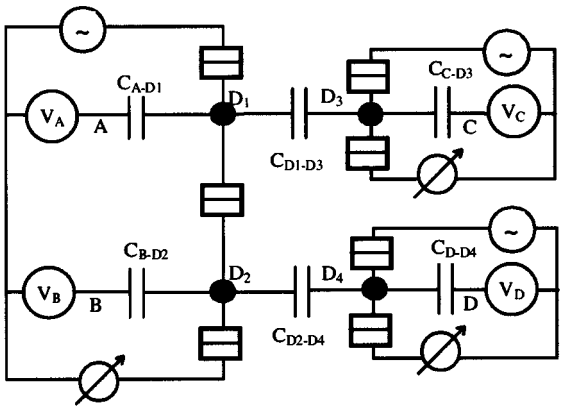

FIG. 2. Schematic diagram of the device structure. The circuit used to compensate for parasitic capacitance between the driver gates A/B and the electrometer islands D_3/D_4 is not shown.

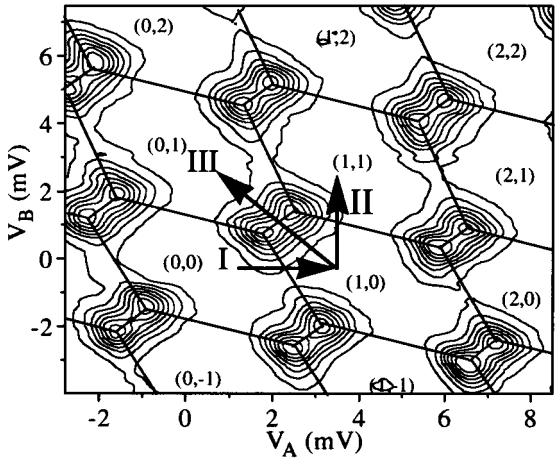

FIG. 3. Charging diagram of the double dot as a function of the gate voltages V_A and V_B. Charge configurations (n_1 and n_2), which represent the number of extra electrons on D_1 and D_2, respectively, are arbitrarily chosen. Lines labeled I, II, and III show a few directions in which charge can shift between different configurations of the double dot.

the Coulomb blockade oscillations (CBO).[1] The double dot structure is used as a gate electrode to measure the capacitance of the coupling capacitors $C_{D_1-D_3}$ and $C_{D_2-D_4}$.

In our experiments, the charge on the double-dot structure is varied by sweeping gates A and B. Conductances through the double dot and both electrometers are measured simultaneously as a function of the control gate voltages. To prevent these voltages from affecting the electrometers due to parasitic capacitance, we apply cancellation voltages, with polarities opposite to V_A and V_B, to gates C and D. Using this charge compensation technique, we can observe up to 100 periods in the electrometer conductances due to discrete variations of the coupled island charges, without inducing extra charge on the electrometers due to the control gates. The operating points of the electrometers are set to be equal to each other on a rising edge of their current versus island charge characteristics to ensure an identical response from each one. We have designed coupling capacitors $C_{D_1-D_3}$ and $C_{D_2-D_4}$ to be relatively large in order to make the electrometers sensitive to small charge variations on the double dot, yet our measurement process is noninvasive since the coupling capacitors constitute only 10% of C_Σ.[15]

The motion of electrons within the double dot can best be understood from its charging diagram. A contour plot of conductance through the double-dot, $G_{\text{double dot}}(V_A, V_B)$, is shown in Fig. 3. The peaks in conductance at triple points, depicted by a convergence of contour lines, form a hexagonal ''honeycomb'' observed by Pothier *et al.*[5] Each hexagonal cell is delineated by solid lines surrounding regions where a particular configuration (n_1, n_2) is the ground state, with n_1 and n_2 representing the number of excess electrons on dots D_1 and D_2, respectively. In the interior of the cell, there is no charge transport through the double dot due to the Coulomb blockade of electrons. Under the influence of control gates, the charge configuration of the double dot can be varied by crossing honeycomb borders along any of the three directions shown in Fig. 2. This does not result in significant current flow through the double dot if the path chosen avoids triple points. Along directions I and II, charge is added to only one of the dots in units of single electrons, while the population of the other dot stays constant. Charge redistribution in the double dot takes place along direction III when electrons transfer from one dot to the other while maintaining the total charge on the double-dot constant.

Figure 4(a) shows a small section of the double-dot charging diagram, along with plots of the conductance through the electrometers D_3, G_{D_3}, and D_4, G_{D_4}, shown in Figs. 4(b) and 4(c), respectively. Lighter areas in these gray scale contour plots represent higher conductance. To demonstrate that a replica of the double-dot charging diagram can be traced in the electrometer signals, we superimpose the honeycomb boundaries from Fig. 4(a) onto Figs. 4(b) and 4(c). The change in the conductance of each electrometer reflects the variation of the electrostatic potential in the dot capacitively coupled to it. A sharp change in the conductance

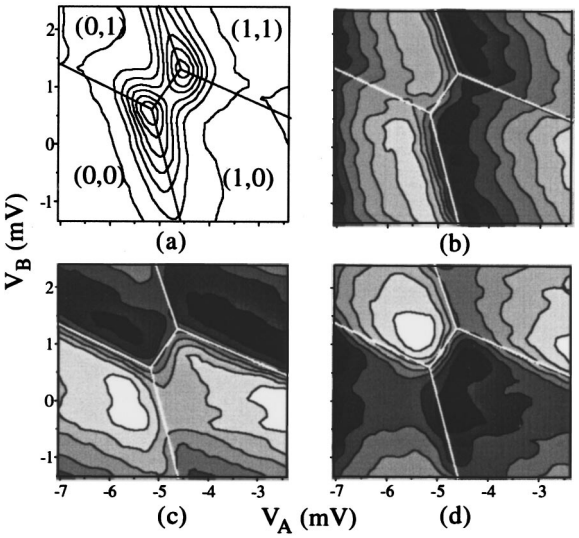

FIG. 4. (a) Smaller section of the double dot charging diagram as a function of gate voltages V_A and V_B. (b) and (c) Conductances of the electrometers D_3 and D_4, respectively, with the honeycomb boundaries of Fig. 4(a) superimposed. Sharp transitions in the horizontal direction in (b) indicate a change in the population of D_1. Sharp transitions in the vertical direction in (c) reflect a change in the population of D_2. (d) Differential signal obtained from the conductances of the individual electrometers.

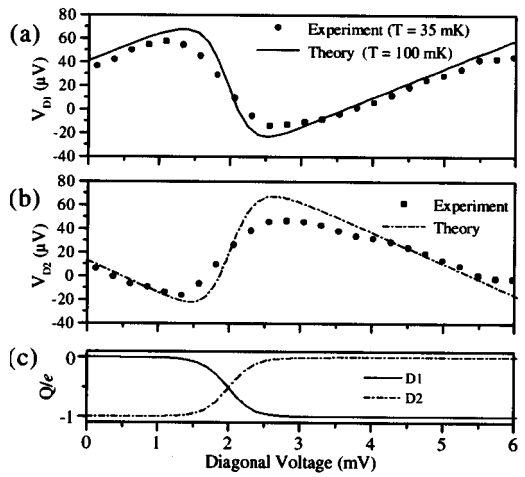

FIG. 5. (a) and (b) Experimental and theoretical curves showing potential changes in dots D_1 and D_2, respectively, during charge redistribution in the double dot. The solid line represents the simulation result at 100 mK, and the dotted line shows the experimental values calculated from the conductances of D_3 and D_4. (c) Theoretical calculations of the charges on dots D_1 and D_2 during charge redistribution.

of D_3 (from light to dark) in the horizontal direction [Fig. 4(b)] represents addition of an electron to D_1. Similarly, sharp variation in conductance of D_4 in the vertical direction [Fig. 4(c)] indicates discrete variation of charge on D_2. Hence, the sharpest variations in the conductances of each electrometer reveal the charging of their capacitively coupled dots.

Sensing the state of a QCA cell requires detection of the polarization change in the double dot shown by direction III in the charging diagram of Fig. 2. In Figs. 4(b) and 4(c), we see that the transitions along this direction are detected less strongly in the electrometer signals. This is due to the cross capacitance between dots $D_1(D_2)$ and $D_4(D_3)$ which makes each electrometer sensitive to both dots. According to our measurements, the sensitivity of the electrometers to the remote dots is about 30% of that to the nearby dots. During charge redistribution in the double dot, the signals from the two electrometers are out of phase by 180° and each reflects the superposition of the two signals. As a result, the detected signal is about 30% weaker than that along direction I (II) in the conductance of $D_3(D_4)$. To show the polarization change of the double dot more prominently, we use the differential signal from the two electrometers, $G_{D_3}-G_{D_4}$, as shown in Fig. 4(d). The most conspicuous transition, represented by a higher density of contour lines, occurs at the boundary between the (0,1) and (1,0) states, indicating an electron shift from one dot to the other. As mentioned above, this is due to the phase difference (180°) in the signals of the individual electrometers, yielding a differential signal which is approximately twice as strong as the one detected by a single electrometer.

We compare the measured potential changes on dots D_1 and D_2 during the charge redistribution in the double dot (direction III in Fig. 3) with theoretical results, which include the experimentally determined capacitance parameters. Figures 5(a) and 5(b) show the experimental and theoretical plots of the potentials on dots D_1 and D_2, respectively, as a function of the ''diagonal voltage,'' where $\Delta V_A=-\Delta V_B$. As expected, the potentials on the two dots change linearly, maintaining a phase difference of 180° with an abrupt shift when the electron populations of the dot change. To confirm that the observed potential change of the two dots is caused by a polarization switch in the double dot, we also show calculated charges on the dots in Fig. 5(c). The theoretical results are obtained by minimizing the classical electrostatic energy for the array of islands and voltage leads. The full capacitance matrix is included, and the minimum energy charge configuration is calculated subject to the condition that island charge be an integer multiple of electronic charge. Finite temperature effects are obtained by performing the thermodynamic averaging over all nearby charge configurations. The experiment matches theory very well with only the substrate background charge and temperature as fitting parameters. The background charge adds an uncontrolled offset to the position of the peaks, but does not change the magnitude or period of the dot potentials. The best fit to experiment is obtained for a temperature of 100 mK. The discrepancy between this and the temperature of the experiment (35 mK) is most likely due to heating of the electron subsystem by the applied 4 μV excitation and insufficient filtering of the leads.

In summary, we have presented direct measurement of the internal state of a coupled dot system by externally detecting all possible charge transitions of a single electron. A polarization change of the double dot is most prominently seen in the differential signal that utilizes the signals from both electrometers. As proposed by Lent *et al.*,[10] a complete implementation of quantum-dot cellular automata requires the detection of single electron motion between dots. With this investigation, we demonstrate that our differential detector can be used to confirm the operation of a QCA cell.

This research was supported in part by DARPA, ONR (Grant No. N0014-95-1-1166) and NSF. The authors wish to thank W. Porod and J. Merz for helpful discussions.

[1] D. V. Averin and K. K. Likharev, in *Mesoscopic Phenomena in Solids*, edited B. L. Altshuler, P. A. Lee, and R. A. Webb (North Holland, Amsterdam, 1991), Chap. 6.
[2] *Single Charge Tunneling*, edited by H. Grabert and M. H. Devoret (Plenum, New York, 1992).
[3] W. P. Kirk and M. A. Reed, *Nanostructures and Mesoscopic Systems* (Academic, Boston, 1992).
[4] F. R. Waugh, M. J. Berry, D. J. Mar, and R. M. Westervelt, Phys. Rev. Lett. **75**, 705 (1995).
[5] H. Pothier, P. Lafarge, C. Urbina, D. Esteve, and M. H. Devoret, Europhys. Lett. **17**, 249 (1992).
[6] T. Sakamoto, S. Hwang, F. Nihey, Y. Nakamura, and K. Nakamura, Jpn. J. Appl. Phys. **33**, 4876 (1994).
[7] J. R. Tucker, J. Appl. Phys. **72**, 4399 (1992).
[8] C. S. Lent, P. D. Tougaw, and W. Porod, Appl. Phys. Lett. **62**, 714 (1993).
[9] P. D. Tougaw, C. S. Lent, and W. Porod, J. Appl. Phys. **74**, 3558 (1993).
[10] C. S. Lent, P. D. Tougaw, W. Porod, and G. H. Bernstein, Nanotechnology **4**, 49 (1993).
[11] C. S. Lent and P. D. Tougaw, J. Appl. Phys. **75**, 4077 (1994).
[12] J. M. Martinis, M. Nahum, and H. D. Jensen, Phys. Rev. Lett. **72**, 904 (1994).
[13] P. D. Dresselhaus, L. Ji, S. Han, J. E. Lukens, and K. K. Likharev, Phys. Rev. Lett. **72**, 3226 (1994).
[14] P. Lafarge, H. Pothier, E. R. Williams, D. Esteve, C. Urbina, and M. H. Devoret, Z. Phys. B **85**, 327 (1991).
[15] G. Bazan, A. O. Orlov, G. L. Snider, and G. H. Bernstein, J. Vac. Sci. Technol. B **14**, 40 (1996).
[16] T. A. Fulton and G. H. Dolan, Phys. Rev. Lett. **58**, 109 (1987).